2009 American Control Conference
Hyatt Regency Riverfront, St. Louis, MO, USA
June 10-12, 2009

Control Design for Force Balance Sensors

Zi Yie, Nitin Kataria, Chris Burgner, Karl Åström, Forrest Brewer, Kimberly Turner

Abstract— **This paper describes a design methodology for force balance sensors and applies it to the design of a tunneling accelerometer. A controller based on feedback from estimated states is a natural basis for the design. It provides a controller with a rich choice of design methods. The feedback gains can be used to tune the motion of the mass but they do not influence the sensor transfer function that is uniquely given by the filter gains. Since low currents and small distances are measured, noise is an important factor. The main contributions are thermal noise from the air molecules hitting the mass, Johnson-Nyquist noise in the input resistor of the transimpedance amplifier, and tunneling noise. The effects of noise are analyzed giving fundamental limitations for the achievable resolution. The properties of the system are illustrated by simulations and experiments.**

I. INTRODUCTION

Force balance is a principle that has been used to improve the performance of sensors for a long time [1]. Feedback design is important because it is the key idea in force balance, but signal processing is also important because the major problem is to obtain a good estimate of a physical quantity. In this paper we will discuss the design of force balance systems. It is shown that such systems can be designed based on a standard configuration with state feedback and an observer. The main idea is to make a mathematical model where the unknown force is a state, and the best estimate is then simply obtained from the observer. An interesting feature of the problem is that the sensor transfer function and the variance of the estimate only depend on the observer gains. A designer thus has considerable freedom in choosing the feedback gains. These results are applied to the design of an accelerometer with feedback from a tunneling sensor.

Although considerable work has been done on the control of tunneling accelerometers in the past, most either did not incorporate uncertainty in the design [2], or have used complicated methods resulting in high order controllers [3], [4]. The force balance control approach used in this paper allows for the design of a simple, robust and low order controller that is both effective and easily implemented. The paper presents analysis, simulation, and practical experiments.

This work was supported by NSF grant CSR-EHS 0720840 and ICB grant W911NF-09-D-0001

Zi Yie, Chris Burgner, Karl Åström and Kimberly Turner are with the Department of Mechanical Engineering, University of California, Santa Barbara, CA

Nitin Kataria and Forrest Brewer are with the Department of Electrical and Computer Engineering, University of California, Santa Barbara, CA

II. MODELING AND SYSTEM DESIGN

We assume that the sensor can be modeled by a linear system

$$\frac{dx}{dt} = Ax + B(u + w) \qquad y = Cx, \tag{1}$$

where x is the state variable, w is the force that we want to measure, u is the control signal, and y is the error signal that we try to keep small. In the model we have assumed that the control signal enters at the same place as the physical variable. Intuitively, the control signal u will be close to the unknown force $-w$ if the output y is small. For simplicity we have normalized u and w so that they have the same units.

To have a complete model, we must also have a model for the dynamics of the signal we want to measure. A simple model is to assume that w is constant but unknown, hence

$$\frac{dw}{dt} = 0. \tag{2}$$

Augmenting the state x with w gives a standard linear model described by the matrices

$$A_a = \begin{bmatrix} A & B \\ 0 & 0 \end{bmatrix} \quad B_a = \begin{bmatrix} B \\ 0 \end{bmatrix} \quad C_a = \begin{bmatrix} C & 0 \end{bmatrix}. \tag{3}$$

A straight forward way to design the system is to use a state feedback and a Kalman filter. The state w is naturally not reachable (we cannot influence the external force), but it is observable if the matrix A does not have an eigenvalue at the origin. The control law then becomes

$$\begin{aligned} \frac{d\hat{x}}{dt} &= A\hat{x} + B(u + \hat{w}) + L(y - C\hat{x}) \\ \frac{d\hat{w}}{dt} &= l(y - C\hat{x}) = l(y - \hat{y}) \\ u &= -\hat{w} - K\hat{x}. \end{aligned} \tag{4}$$

The controller transfer function is

$$H(s) = \frac{l}{s} - \frac{lC + K}{s}[sI - A + BK + LC]^{-1}L.$$

The controller always has an integral action. Also notice that if $K = 0$, the controller reduces to

$$H(s) = \frac{l}{s}(1 - C[sI - A + LC]^{-1}L).$$

This transfer function has poles at $s = 0$ and at the eigenvalues of $A - LC$ and zeros at the eigenvalues of A, which means that it can be interpreted as an integrator combined with a notch filter that filters out the system dynamics.

978-1-4244-4524-0/09/$25.00 ©2009 AACC

A. Sensor Resolution

Sensor resolution is given by the noise in the system and the character of the variations in the physical variable. Assuming that the disturbances can be captured by stochastic models, we can determine the variance of the estimated variable by using stochastic control techniques. Assuming that the system and its environment are modeled by

$$\begin{aligned} dx &= A_a x dt + B_a u dt + dv \\ dy &= C_a x dt + de, \end{aligned} \tag{5}$$

where x is now the augmented state, A_a, B_a and C_a are the augmented system matrices, and v and e are Wiener processes with incremental covariances $R_x dt$ and $R_y dt$. The steady-state covariance of the best estimates is given by

$$A_a P + P A_a^T + R_x - P C_a^T R_y^{-1} C_a P = 0, \tag{6}$$

and the variance of the measured variable is then

$$\sigma_{\hat{w}}^2 = C_w P C_w^T, \tag{7}$$

where C_w is the vector that picks out w from the augmented state. Notice that the variance of the estimate does not depend on the feedback gains.

The steady-state filter gains are given by

$$L_a = \begin{bmatrix} L \\ l \end{bmatrix} = P C_a^T R_y^{-1}. \tag{8}$$

B. Sensor Transfer Function

The sensor transfer function $G_{\hat{w}w}(s)$ relates the estimate $\hat{w}$ of the physical quantity to its real value w. To find this transfer function, we introduce x, $\tilde{x} = x - \hat{x}$, and $\hat{w}$. The equation then becomes

$$\begin{aligned} G_{\hat{w}w}(s) &= \begin{bmatrix} 0 & 1 \end{bmatrix} \begin{bmatrix} sI - A + LC & -B \\ -lC & s \end{bmatrix}^{-1} \begin{bmatrix} B \\ 0 \end{bmatrix} \\ &= \frac{lC(sI - A + LC)^{-1}B}{s + lC(sI - A + LC)^{-1}B}. \end{aligned} \tag{9}$$

Notice that the sensor transfer function $G_{\hat{w}w}(s)$ depends on the filter gains l and L but not on the feedback gains K. This implies that we have considerable freedom in choosing the feedback gains.

C. Design

There are many control theories that give a controller of the form in (4), and there are many methods that can be used to obtain the filter gains l and L and the feedback gains K. Which method we choose depends on the particular information available and the nature of the sensor. Noise is often a fundamental limitation as illustrated by (7) and it is then natural to apply stochastic control theory [5]. A key difficulty is to obtain information about the nature of variations in the physical quantity that we want to measure. In other situations the key difficulty may be due to parameter variations and it is then natural to use robust control theory [6], [7], [8]. If the properties of the signal we want to measure are not well known, a reasonable solution is to design the instrument for a given bandwidth of the transfer function $G_{\hat{w}w}(s)$ shown in (9). The bandwidth can even be brought to the front panel of the instrument as a user adjustable parameter.

III. A Tunneling Accelerometer

We will now consider a specific case, namely a tunneling accelerometer. Figure 1 shows the accelerometer chip which is described in [9]. For our experiment the chip was provided with improved electronics, where a new preamplifier was built and interfaced with a National Instruments CompactRIO platform.

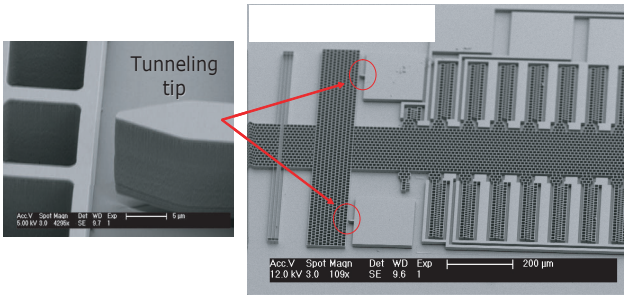

Fig. 1. Picture of the accelerometer chip (right) and zoomed-in view of the tunneling tip (left), from [9].

A. Preamplifier

Since our goal was to measure a tunneling current on the order of 2 nA with a minimum amount of noise and over a large bandwidth of 5 kHz, we built a custom transimpedance preamplifier. The preamplifier was built using Texas Instruments OPA656 ultra-low noise op-amps and was configured such that the input impedance of the first stage was set to 10.2 MΩ while a voltage gain of 2 was provided by the second stage. The preamplifier was built on a custom printed circuit board and was housed in an electromagnetically shielded box. Batteries were used to power the preamplifier in order to keep the noise levels low. Under test conditions, the preamplifier generated about 3 mV of peak-to-peak noise. Figure 2 shows a block level diagram of the preamplifier. The "bias" input is used to provide a constant bias for the tunneling junction.

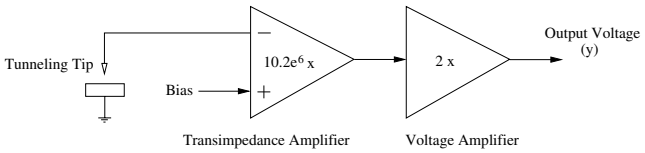

Fig. 2. Block diagram of the preamplifier.

B. Accelerometer System

Figure 3 shows a block diagram of the accelerometer system.

There are four blocks representing the comb-drive actuator, the mass system, the tunneling tip and the amplifier. The

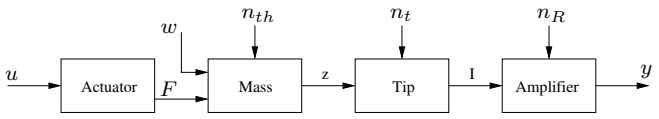

Fig. 3. Block diagram of the accelerometer system.

input u is the control signal and the output y is the equivalent output voltage from the tunneling tip.

It is straight forward to model the system. The essential nonlinearities are in the comb-drive actuator and the tunneling tip. Most coefficients can be obtained from physics, while the resonant frequency ω_0 and the Q value can be obtained by simple experiments. Sensor noise characteristics can also be obtained from physics. Tunneling is a very sensitive way of measuring displacement, the resolution is a fraction of an Ångström. Since the tunneling current is on the order of a few nanoamperes, the design of the sensing amplifier is a critical issue.

C. Modeling

Since the position of the mass is controlled accurately, the control design can be done using linearized models. The following model based on [9] will be used

$$\begin{aligned}
&\text{Actuator:} && F = k_a u \\
&\text{Mass:} && m\ddot{z} + c\dot{z} + kz = F - mw + n_{th} \\
&\text{Tunneling tip:} && I = k_t z + n_t \\
&\text{Amplifier:} && y = k_v(RI + n_R) \\
&\text{Acceleration:} && \dot{w} = n_w,
\end{aligned}$$

where the variables denote deviations from reference values. The actuator model is a static model which is obtained by linearizing the nonlinear model. A standard mass-damper-spring model is used for the mass system. The model for the tunneling tip is also obtained by linearizing the nonlinear model, where the tunneling gain k_t depends on the tunneling current. It is assumed that the amplifier for the tunneling current has two stages. The first stage has an effective feedback resistance R, and the second stage has a voltage gain k_v. The dynamics of the amplifier are neglected. The main disturbances are the thermal noise n_{th} acting on the mass, the tunneling noise n_t, and the resistor noise n_R. The characteristics of these noise sources are obtained from physics which will be discussed later.

Comparing with the general model given by (1) we find that the scaling of u is k_a/m, where k_a [N/V] is the actuator gain. The parameter k_a is essential for the calibration of the sensor. Since the comb-drive actuator is nonlinear, it may be worthwhile to introduce the nonlinear model for the actuator.

Modeling the variations of the quantity that we intend to measure is a major issue. The model in (2) implies that the acceleration is constant but unknown. A simple stochastic model is to assume that it is a Wiener process, which can be represented as (2) driven by white noise with the spectral density n_w. A more elaborate model would be to assume that the spectral density or other characteristics of the acceleration are known.

TABLE I
SYSTEM PARAMETERS

Boltzmann's constant	k_B	1.38×10^{-23} J/K
Charge of electron	q_0	1.6×10^{-19} C
Temperature	T	293 K
Mass	m	4.917 µg
Resonant frequency	f_0	4.2 kHz
Q-value	Q	10
Actuator gain	k_a	9.2×10^{-7} N/V
Tunneling gain	k_t	4 A/m
Preamp resistance	R	10.2 MΩ
Voltage gain	k_v	2

The parameters of the system are based on the system in [9]. The numerical values are given in Table I.

D. A Low Bandwidth Sensor

The complexity of the model depends on the requirements of the system. We will start with the situation when a low bandwidth system is needed. If the bandwidth of the system is significantly smaller than the resonant frequency ω_0, the dynamics of the mass system can be neglected and the model can be represented by the static model

$$y = \frac{mk_s}{k}\Big(\frac{k_a}{m}u - w\Big) = \frac{k_s}{\omega_0^2}\Big(\frac{k_a}{m}u - w\Big) = C_a\Big(\frac{k_a}{m}u - w\Big), \tag{10}$$

where $k_s = k_v k_t R$. The state is the acceleration w that we want to measure.

Comparing with (1), the system has a direct term because the sensor dynamics were approximated by a static model. The augmented system in (5) has one state and the incremental covariances of v and e are given by

$$\begin{aligned}
r_y &= 2ck_BT\Big(\frac{k_v k_t R}{k}\Big)^2 + q_0 I_0 (k_v R)^2 + 2k_B T R k_v^2 \\
r_x &= r_w.
\end{aligned} \tag{11}$$

Since $A_a = 0$ the Riccati equation in (6) reduces to

$$r_x - PC_a^T r_y^{-1} C_a P = 0,$$

which has the solution

$$P = \sqrt{r_x r_y}/C_a. \tag{12}$$

Since the only state is the disturbance state w we have $L_a = l$, and the filter gain is $L_a = PC_a^T R_y^{-1} = \sqrt{r_w/r_y}$. The controller that minimizes the fluctuation is given by

$$u = \frac{m}{k_a}\hat{w} \tag{13}$$

and the Kalman filter becomes

$$\frac{d\hat{w}}{dt} = L_a\Big(y - C_a\Big(\frac{k_a}{m}u - \hat{w}\Big)\Big) = ly, \tag{14}$$

where the last equality follows from (13). The controller is simply an integrating controller of the form

$$u = \frac{m}{k_a}\hat{w} = \frac{ml}{k_a}\int_0^t y(\tau)d\tau. \tag{15}$$

The observer has the bandwidth

$$\omega_B = L_a C_a = C_a \sqrt{\frac{r_w}{r_y}} = \frac{k_s}{\omega_0^2}\sqrt{\frac{r_w}{r_y}}. \tag{16}$$

Notice that r_w/r_y can be interpreted as a signal-to-noise ratio. Equation (16) thus implies that the bandwidth of the filter is proportional to the square root of the signal-to-noise ratio.

The variance of the acceleration estimate is

$$\begin{aligned} P &= \frac{\sqrt{r_w r_y}}{C_a} = \frac{1}{C_a}\sqrt{\frac{r_w}{r_y}} r_y = \frac{\omega_B r_y}{C_a^2} = P_{th} + P_t + P_R \\ &= \frac{\omega_B}{m^2}\Big(2ck_BT + \frac{q_0 I_0 k^2}{k_t^2} + \frac{2k_B T k^2}{k_t^2 R}\Big), \end{aligned} \tag{17}$$

where P_{th}, P_t, and P_R represent the contributions due to thermal noise, tunneling noise and resistor noise, respectively. The term corresponding to thermal noise is

$$P_{th} = \frac{2\omega_B c k_B T}{m^2} = \frac{2\omega_B \omega_0 k_B T}{mQ}. \tag{18}$$

The ratios of the different noise sources are

$$\begin{aligned} \frac{P_R}{P_{th}} &= \frac{m\omega_0^3 Q}{k_t^2 R} (\approx 0.03) \\ \frac{P_t}{P_R} &= \frac{q_0 I_0 R}{2k_B T} (\approx 0.08), \end{aligned}$$

where the numbers indicate that the major contribution is due to the thermal noise.

It follows from (10) that the system transfer function is $G(s) = C_a = k_s/\omega_0^2$ and (9) then gives the sensor transfer function as

$$G_{\hat{w}w}(s) = \frac{L_a C_a}{s + L_a C_a} = \frac{\omega_B}{s + \omega_B}, \tag{19}$$

where

$$\omega_B = L_a C_a = \frac{k_v k_t R m}{k}\sqrt{\frac{r_w}{r_y}},$$

if the dynamics of the mass system are neglected, and

$$\begin{aligned} G_{\hat{w}w}(s) &= \frac{L_a C_a}{s\Big(1 + \frac{c}{k}s + \frac{m}{k}s^2\Big) + L_a C_a} \\ &= \frac{\omega_B \omega_0^2}{s^3 + 2\zeta_0\omega_0 s^2 + \omega_0^2 s + \omega_B \omega_0^2}, \end{aligned} \tag{20}$$

if the dynamics of the mass system are included.

It follows from the Routh-Hurwitz criterion that the system is stable if $\omega_B < 2\zeta_0\omega_0 = \omega_0/Q$. The possible bandwidth is

$$\omega_B \le \frac{2\zeta_0\omega_0}{g_m} = \frac{\omega_0}{g_m Q} \tag{21}$$

if we require a gain margin of g_m.

Figure 4 shows the Bode plots of the transfer function $G_{\hat{w}w}(s)$ for $\zeta_0 = 0.05$ ($Q = 10$) and different ratios of ω_B/ω_0.

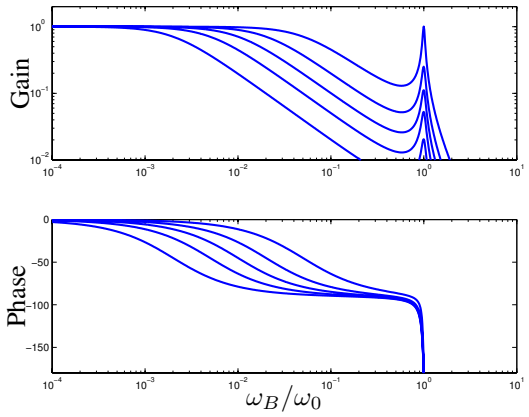

Fig. 4. Bode plots of the sensor transfer function $G_{\hat{w}w}(s)$ for $\zeta_0 = 0.05$ ($Q = 10$) and $\omega_B/\omega_0 = 0.002$, 0.005, 0.01, 0.02, and 0.05.

IV. A High Bandwidth Sensor

The simple integrating controller given by (15) is not able to provide an instrument bandwidth larger than $\omega_0/(g_m Q)$. To obtain a high bandwidth system it is necessary to take the mass dynamics into account. Assuming that all the noise sources are white, we find that the system can be modeled as a third-order stochastic differential equation. One state is the unknown acceleration and the other states are the position and the velocity of the mass. Choosing the state variables $x_1 = z$, $x_2 = \dot{z}$ the system matrices become

$$\begin{aligned} A &= \begin{bmatrix} 0 & 1 \\ -k/m & -c/m \end{bmatrix} \qquad B = \begin{bmatrix} 0 \\ 1 \end{bmatrix} \\ C &= \begin{bmatrix} k_s & 0 \end{bmatrix} \qquad D = 0, \end{aligned} \tag{22}$$

where $k_s = k_v k_t R$ and the control signal is scaled with m/k_a. It is assumed that the acceleration to be measured is a Wiener process, and the incremental covariance of the acceleration is $r_w\,dt$ [$\mathrm{m^2 s^4}$]. The disturbance acting on the mass is thermal noise which is represented by a white noise source with spectral density $4ck_BT\,dt$ [$\mathrm{N^2/Hz}$], where $k_B = 1.38 \times 10^{-23}$ [J/K] is Boltzmann's constant and T is the absolute temperature. The Wiener process v representing state noise has the incremental covariance $R_x\,dt$ where

$$R_x = \mathrm{diag}(0\,,\, 2ck_BT/m^2,\ r_w). \tag{23}$$

The measurement noise in (22) is a combination of tunneling noise and resistor noise. Tunneling noise is white with the spectral density $\Phi_t = 2q_0 I_0 \delta(t)$ [$\mathrm{A^2/Hz}$], where $q_0 = 1.6 \times 10^{-19}$ [C] is the charge of the electron and I_0 is the tunneling current. The corresponding incremental covariance is $r_t\,dt$ with $r_t = \Phi_t/2$ [$\mathrm{A^2 s}$]. The tunneling current is amplified by the gain Rk_v, where R is the input resistance in the first stage of the amplifier and k_v is the gain of the second stage. Resistor noise is modeled as Johnson-Nyquist noise which has the spectral density $4k_BTR$ [$\mathrm{V^2/Hz}$]. The corresponding incremental covariance is $r_R\delta(t)$ where $r_R = 2k_BTR$ [$\mathrm{V^2 s}$]. Resistor noise is amplified by the factor k_v in the second stage of the amplifier. Measurement noise is

thus characterized by a Wiener process with the incremental covariance $R_y\,dt$ where

$$R_y = k_v^2(r_R + R^2 r_t) = k_v^2(2k_B T R + R^2 q_0 I_0). \tag{24}$$

The augmented system is third-order and the controller is given by (4) and the filter gains are given by (8). We have

$$\begin{aligned} G(s) &= \begin{bmatrix} k_s & 0 \end{bmatrix} \begin{bmatrix} s + k_s l_1 & -1 \\ k_s l_2 + k/m & s + c/m \end{bmatrix}^{-1} \begin{bmatrix} 0 \\ 1 \end{bmatrix} \\ &= \frac{k_s}{s^2 + s(k_s l_1 + c/m) + k_s(l_1 c/m + l_2) + k/m}, \end{aligned}$$

and it follows from (9) that the sensor transfer function is

$$G_{\hat{w}w}(s) = \frac{l k_s}{a(s)} \tag{25}$$

where

$$\begin{aligned} a(s) &= s^3 + s^2(k_s l_1 + c/m) \\ &\quad + s\big(k_s(l_1 c/m + l_2) + k/m\big) + l k_s. \end{aligned}$$

Notice that the system transfer function $G(s)$ does not depend on the feedback gain K.

To obtain a good frequency response we require that the denomiantor $a(s)$ in (25) to be

$$(s + \alpha_c \omega_c)(s^2 + 2\zeta_c \omega_c s + \omega_c^2).$$

The shape of the frequency response is given by the parameters α_c and ζ_c and the bandwidth is given by ω_c. The filter gains then becomes

$$\begin{aligned} l &= \frac{\alpha_c \omega_c^3}{k_v k_t R} = \frac{\alpha_c \omega_c^3}{k_s} \\ l_1 &= \frac{(\alpha_c + 2\zeta_c)\omega_c - c/m}{k_v k_t R} = \frac{(\alpha_c + 2\zeta_c)\omega_c - 2\zeta_0 \omega_0}{k_s} \\ l_2 &= \frac{(1 + 2\alpha_c \zeta_c)\omega_c^2 - k/m - \big((\alpha_c + 2\zeta_c)\omega_c - c/m\big)c/m}{k_v k_t R} \\ &= \frac{(1 + 2\alpha_c \zeta_c)\omega_c^2 - \omega_0^2 - 2\zeta_0 \omega_0((\alpha_c + 2\zeta_c)\omega_c - 2\zeta_0 \omega_0)}{k_s}, \end{aligned} \tag{26}$$

where $\omega_0 = \sqrt{k/m}$ and $\zeta_0 = c/(2m\omega_0)$. Notice that the filter gain l increases with the third power of ω_c and that l_1 and l_2 approximately increases with the first and second power of ω_c, respectively.

Bode plots of the frequency response for different ratios of ω_c/ω_0 are shown in Figure 5. A comparison with Figure 4 shows that there is a significant improvement.

The controller is given by

$$\begin{aligned} \frac{k_a}{m} u &= -\hat{w} + \bar{u} = -\hat{w} - k_1 \hat{x}_1 - k_2 \hat{x}_2 \\ d\hat{x}_1 &= \hat{x}_2\,dt + l_1(dy - k_s \hat{x}_1\,dt) \\ d\hat{x}_2 &= -(k/m)\hat{x}_1\,dt - (c/m)\hat{x}_2\,dt + \bar{u}\,dt \\ &\quad + l_2(dy - k_s \hat{x}_1\,dt) \\ d\hat{w} &= l(dy - k_s \hat{x}_1\,dt). \end{aligned} \tag{27}$$

The sensor transfer function in (9) is determined by the filter gains l, l_1, and l_2. The feedback gains k_1 and k_2 determine how well the mass is kept to its center position. Their values

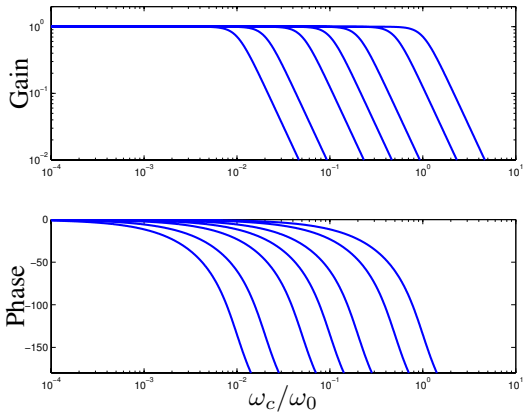

Fig. 5. Bode plots of the sensor transfer function $G_{\hat{w}w}(s)$ for $\omega_c/\omega_0 =$ 0.01, 0.02, 0.05, 0.1, 0.2, 0.5, and 1.

will not influence the sensor transfer function as long as the deviations are so small that the linear approximation is valid. There are many ways to determine the feedback gains k_1 and k_2, using pole assignment, LQG or robust control. In this particular case, with reasonable designs we found that k_1 is essentially zero and therefore we can simply set it to zero. However k_2 is crucial because it influences the damping. After some adjustment of the gains, we found the gains to be $k_1 = 0$ and $k_2 = 3.69 \times 10^4$. These values can be compared with the values of $k/m = 6.96 \times 10^8$ and $c/m = 2.64 \times 10^3$.

A block diagram of the controller with the equations given by (27) is shown in Figure 6.

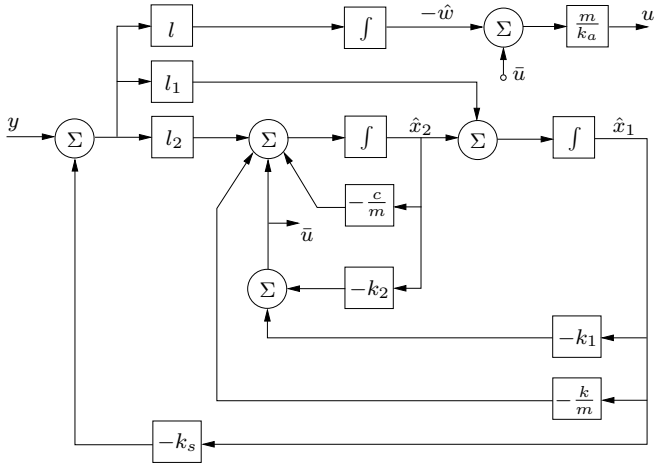

Fig. 6. Block diagram of the controller.

If the feedback gains are zero, we have $\bar{u} = 0$, and the controller can be interpreted as a second-order notch filter in cascade with an integrator. The notch filter attenuates the resonant mode of the mass. The feedback gain k_2 damps the oscillatory mode and the gain k_1 changes its frequency.

Step responses of the linearized model system without noise are shown in Figure 7. The controller is based on a high bandwidth given by the parameters $\omega_c = \omega_0$, $\alpha_c =$

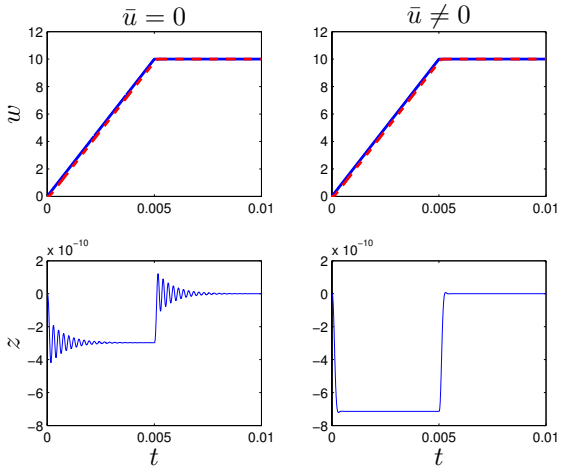

Fig. 7. Step response simulations. The left side shows results for $\bar{u} = 0$. The upper plots show that the acceleration (blue solid) is well tracked by the estimate (red dashed) even if the mass oscillates. The right side shows a design with $\bar{u} = -3.69 \times 10^4 \hat{x}_2$. The oscillations of the mass are now damped.

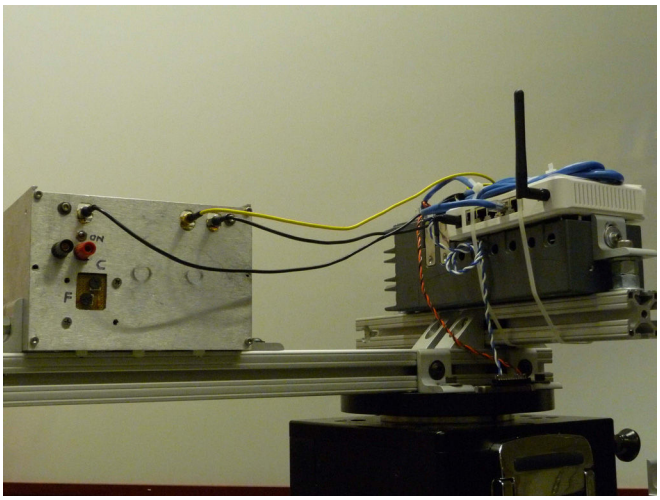

Fig. 8. Experimental set-up. The accelerometer and the CompactRIO are mounted on the rate table. A wireless router connects to the CompactRIO and sends all signals to the PC.

0.75 and $\zeta_c = 0.7$. The filter gains are $l = 1.69 \times 10^5$, $l_1 = 6.63 \times 10^{-4}$, and $l_2 = 7.21$. The feedback gains are $k_1 = 0$ and $k_2 = 3.69 \times 10^4$.

A rate-limited step input having a rise time 5 ms and an amplitude of 10 m/s^2 was used in the simulation. This input is similar to the one that we used in the experiments. Notice that the response of the mass is highly oscillatory for the case $\bar{u} = 0$. The oscillations do not appear in the acceleration estimate because of the actions of the notch filter. The oscillations can be damped by setting $\bar{u} \neq 0$.

V. Experiments

The control algorithm was implemented on a National Instruments CompactRIO platform, which has a field-programmable gate array (FPGA) and a PowerPC host processor with plug-in cards for interfacing with the analog components. The plug-in cards comprise of high bandwidth, 16-bit analog-to-digital and digital-to-analog converters, which communicate with the FPGA through dedicated communication interfaces. The FPGA and the host processor were programmed through the LabVIEW software environment. In our case, the real-time constraints of the control algorithm required us to implement the control computations in the FPGA. The host processor was used to store and display the real-time data, which was received from the FPGA through a direct memory access channel.

The output voltage of the transimpedance preamplifier was sampled by the controller, running on the CompactRIO, to generate the appropriate control action. The bandwidth of the transimpedance preamplifier was adjusted to correspond to the control loop bandwidth chosen for a given implementation. The gain of the preamplifier was chosen to correspond to a 20 mV of DC output for a nanoampere of tunneling current.

To test the system, it was placed on a rate table with computer controlled velocity and acceleration. Figure 8 shows the experimental set up. The CompactRIO was also placed on the rate table and the signals were transferred to the computer through a wireless router. The picture shows the preamplifier box on the left and the compactRIO with the router on the right. The preamplifier was built on a printed circuit board using ultra-low noise op-amps and operated with batteries. The accelerometer was mounted directly onto the printed circuit board itself.

The control algorithm, which is a third-order Kalman filter, was implemented on the FPGA using scaled fixed-point arithmetic. For numerical reasons, a scaled version of the Kalman filter was implemented where all the state variables were scaled appropriately. In particular, the states corresponding to estimated acceleration and displacement were scaled to have the dimensions of voltages. A sampling period of 25 µs was chosen based on the bandwidth of the control loop and the preamplifier roll-off. Besides the Kalman filter, a slow integrating stage with a small gain was implemented to ensure that the mass would safely approach the tunneling tip. A hysteresis loop was also used to switch between the two stages of the controller (slow approach and normal operation as the Kalman filter) when the appropriate tunneling current was detected. It is important to note that the hysteresis loop is only used to switch between the control stages, therefore, at any given time, either the slow approach (slow integrating stage) or the Kalman filter is active. When the Kalman filter is active, hysteresis has no effect on the dynamics of the system performance.

The accelerometer was initialized by giving a constant setpoint of 40 mV for the output of the transimpedance preamplifier. Figure 9 shows the control signal and the output voltage of the preamplifier in the initialization phase. The

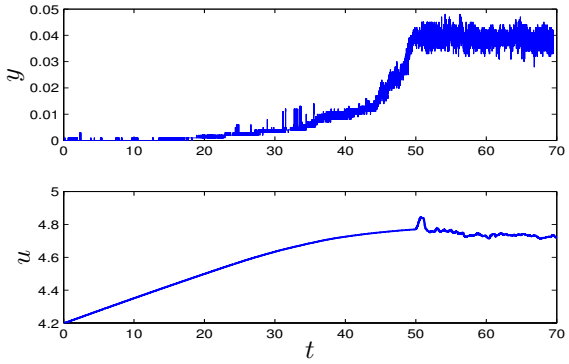

Fig. 9. Initialization of the accelerometer. The upper curve shows the output of the signal preamplifier y in [V], and the lower curve is the control signal u in [V]. The setpoint of the controller is 40 mV, which corresponds to a tunneling current of 2 nA. The time axis t is in seconds.

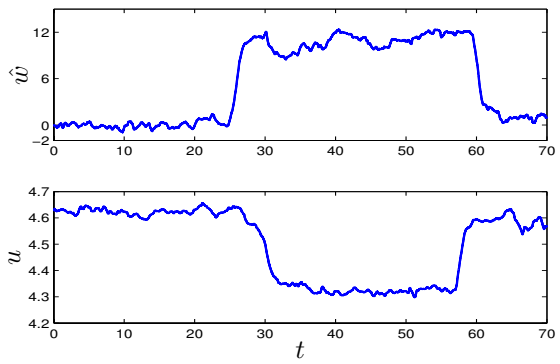

Fig. 10. Response of the accelerometer to a sudden increase of the velocity of the rate table. The upper curve shows the change in estimated acceleration $\hat{w}$ in [m/s^2] relative to the setpoint. The setpoint value is achieved when tunneling starts. The lower curve shows the control signal u in [V]. The time axis t is in seconds.

output voltage is initially small because tunneling does not occur. The variations are due to resistor and amplifier noise. The output voltage starts to increase as the mass approaches the tip and tunneling begins. Simultaneously, the controller gain l is increased and the controller starts to act. The variations in the signal are dominated by the effects of the motion caused by the air molecules hitting the mass. The controller is able to keep the mass close to the desired position. The peak-to-peak variations of the amplifier output y is 18 mV corresponding to a standard deviation of 3 mV, which is equivalent to a position deviation of 0.3 Å. The accelerometer is initialized in such a way that the tip is approximately 1 µm from the mass. The output voltage is essentially the resistor noise because there is no tunneling. The mass is made to move slowly towards the tip by using a low value of the filter gain l. Notice the exponential increase in the tunneling current which reflects the exponential dependence of tunneling current on distance. When tunneling starts, the gain l is switched to the design value and the controller then keeps the output voltage constant. The thermal motion of the mass is now sensed by the tunneling current and the variations in the output signal are now larger.

Once the accelerometer was operational, a step input was then applied by spinning the rate table at a constant rate. Figure 10 shows the estimated acceleration and the control signal. A signal corresponding to 10 m/s^2 was commanded. A change of 0.33 V in control voltage corresponded to about 10 m/s^2 in estimated acceleration.

VI. Conclusions

A general approach for design of force balance sensors, based on feedback from the states of an observer, is presented. Noise analysis is used to find the resolution of the sensor and a feedback controller that gives a good frequency response is designed. The controller implementation is carried out on an FPGA. The results are applied to a tunneling accelerometer and verified by experiments. The analysis is based on a linear model. Since there are nonlinearities in the actuator and the tunneling current, it may be useful to introduce compensation for these effects. The actuator nonlinearity can be compensated by inverting the nonlinearity through a square root function, which can be included in the digital controller. The exponential characteristic of the tunneling current can be compensated by building a logarithmic preamplifier. Future work includes adding such compensations and characterizing the device with the new control system.

VII. Acknowledgments

The authors gratefully acknowledge the contribution of Laura Oropeza-Ramos, who fabricated tunneling accelerometer chips, and provided preliminary data on the device characteristics and an integrating controller. The authors also wish to thank Jeannie Falcon, Javier Gutierrez, and Brian MacCleery at National Instruments for their valuable support on LabVIEW and the CompactRIO platform.

References

[1] B. Liptak. *Instrument Engineers' Handbook: Process Measurement and Analysis*. CRC Press, New York, 2003.

[2] J. Wang, Y. J. Zhao, T. H. Cui, and K. Varahramyan. Synthesis of the modeling and control systems of a tunneling accelerometer using the matlab simulation. *Journal of Micromechanics and Microengineering*, 12:730–35, 2002.

[3] C. H. Liu, H. K. Rockstad, and T. W. Kenny. Robust controller design via u-synthesis for high-performance micromachined tunneling accelerometers. In *Proceedings of the American Control Conference, San Diego, CA*, 1999.

[4] M. Khammash, L. A. Oropeza-Ramos, and K. L. Turner. Robust feedback control design of an ultra-sensitive, high bandwidth tunneling accelerometer. In *Proceedings of the American Control Conference, Portland, OR*, 2005.

[5] K. J. Åström. *Introduction to Stochastic Control Theory*. Dover, New York, 2006. Reprint. Originally published by Academic Press 1970.

[6] K. Zhou and J. C. Doyle. *Essentials of Robust Control*. Prentice Hall, Upper Saddle River, NJ, 1998.

[7] G. C. Goodwin, S. F. Graeve, and M. E. Saldago. *Control System Design*. Prentice Hall, Upper Saddle River, NJ, 2001.

[8] B. Friedland. *Control System Design: An Introduction to State-Space Methods*. Dover, New York, 2006.

[9] L. A. Oropeza-Ramos, N. Kataria, C. B. Burgner, K. J. Åström, F. Brewer, and K. L. Turner. Noise analysis of a tunneling accelerometer based on state space stochastic theory. In *Solid-State Sensor, Actuator, and Microsystems Workshop, Hilton Head, SC*, 2008.